Autonomous Navigation via Visual Servoing with a Hybrid Sensor System

Jie Liang Choo, Nur Syazreen Ahmad*, and Patrick Goh
School of Electrical & Electronic Engineering, Universiti Sains Malaysia, 14300 Nibong Tebal, Penang, Malaysia
Email: choojieliang@student.usm.my, syazreen@usm.my*, eepatrick@usm.my

***Abstract*— In this work, a framework for a hybrid sensor system is proposed to improve the visual servoing technique of an autonomous wheeled mobile robot. The system consists of an image sensor which is mounted on the robot's robotized head and a range sensor which is fixed at the front position of the robot. The image sensor has the capability to extract the features from a 2D image but is bound to lose its detection when the distance between the sensor and the target image is too close. The range sensor, on the other hand, has the limitation of unstable detection when the target object is too far or/and not in the line of sight, but is useful when the target object is sufficiently close. Two mini nonholonomic robots are used as the test beds and a set of experiments is designed in this work to investigate the impacts of the hybrid sensor system on the tracking performance of the robot. With the speed of the robots constrained within ±20 cm/s, and the distance between them not more than 40cm, it is shown that both sensors compensate each other's limitations in order to ensure the tracking performance is within the design requirement.**

***Index Terms*—visual servoing, autonomous, hybrid sensor**

I. Introduction

Vision-based robotic systems in the early days operated in an open-loop manner via a technique called static-look-then-move [1]. Position loop was then introduced in the outer feedback to improve the accuracy of the system. This approach is now well-known as visual servoing, which, in general, is defined as a technique where the motion of a robot is controlled based on the feedback from a vision sensor [2]. Over the decades, this method expands rapidly in numerous fields and has been extensively used in motion control for robot manipulators and mobile robotics.

Two most common visual servoing techniques are Image-Based Visual Servoing (IBVS) and Position-Based Visual Servoing (PBVS). In IBVS, a target feature is extracted directly from the image itself, without any image interpretation. Features that are obtained from the images are usually primitives like ellipsis, lines, points or moments, and the corresponding error is generated directly from the image plane features [3-4]. Since it is in 2D only, there is no necessity in reconstructing 3D features of the image, thus these images are usually primitives like ellipsis, lines, points or moments, and the corresponding error is generated directly from the image plane features [3-4]. approach allows low processing time and higher sampling rate. The robot will only need to move until the current image features converge to their desired values. Nevertheless, there are some issues related to IBVS technique such as local minima [5], and the problem when the target object falls out of range. Furthermore, when the object has a large rotational angle, the system may not recognize the object and consequently amplify the tracking error.

In PBVS, features that are extracted directly from the 2D image are transposed into a 3D Cartesian space to situate the object in real world, thus it is also termed as 3D visual servoing. Kinematic errors will also be generated in the 3D Cartesian space and mapped to actuator commands [6]. Although it is prone to image sensor calibration errors, target model accuracy, and image measurement noise, the accuracy is relatively higher than the IBVS technique. Hence it is typically used for camera calibration, object recognition, visual odometry and photogrammetry [7].

In automotive field industry, autonomous vehicles that are integrated with PBVS technique usually work as navigation and guidance robots or cars. This technique has a distinctive advantage as compared to the dead-reckoning approach as it can bypass the problem of error accumulation due to inaccurate modeling of the environments as well as wheel slippage [8]. The aforementioned problem is alleviated as PBVS does not need absolute positioning of both the goal and the robot itself. Hence, PBVS may also be a better option for robot navigation in unknown and unreachable areas with various missions.

In practice, however, the success of PBVS technique when applied to wheeled mobile robots for autonomous navigation highly depends on the accuracy of the vision sensor as well as the control strategy. In this work, a framework for a hybrid sensor system is proposed to improve the PBVS technique of an autonomous wheeled mobile robot. The system consists of an image sensor which is mounted on the robot's robotized head and an IR sensor which is fixed at the front position of the robot. The image sensor has the capability to extract the features from a 2D image but is bound to lose its detection when the distance between the sensor and the target image is too close. The range sensor, on the other hand, has the limitation of unstable detection when the target object is

Manuscript received July 1, 2019; revised May 7, 2020.

doi: 10.18178/ijmerr.9.6.906-910

too far or/and not in the line of sight, but is useful when it is sufficiently close. Two mini nonholonomic robots are used as the test beds and a set of experiments is designed in this work to investigate the impacts of the hybrid sensor system on the tracking performance of the robot. With the speed of the robots constrained within ±20 cm/s, and distance between them not more than 40cm, it is shown that both sensors compensate each other's limitations in order to ensure the tracking performance is within the design requirement.

II. Methodology

In this work, two mini nonholonomic robots are used as the test beds where one is set to be the leader (Robot L) and another is set to be the follower robot (Robot F). The dimensions of both robots are approximately *14cm x 10cm x 10cm* (*width x length x height*). Robot L will be independently controlled by the user, and Robot F is tasked to track and follow Robot L from the back within a specified range. An IR sensor (S1) and an image sensor (S2) are mounted at the front of Robot F and a reference image (R1) is placed at the back of Robot L as illustrated in Fig. 1. S2 is also connected to a servo motor to form a robotized vision head which can move to the right or to the left with a maximum of 90° from the center. The variable *d* is the distance between Robot F and Robot L that will be directly detected by S1, while for S2, the data that will be received is the position of R1 in terms of *x*,*y* and *m* as depicted in Fig. 2.

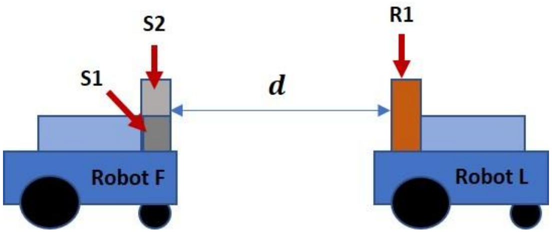

Figure 1. Illustration on the robots' configurations, the sensors' positions and the reference.

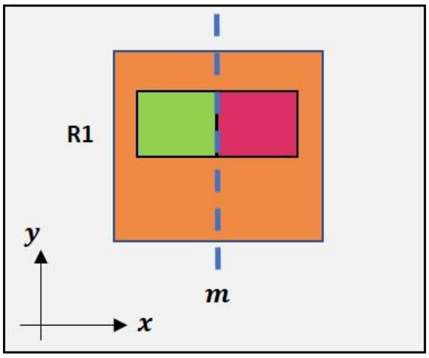

Figure 2. Front view of the reference image, R1.

In Fig. 2, the grey background represents the view field of Robot F if Robot L is placed at its front as illustrated in Fig. 1. The default reference coordinates of top left, top right, bottom left, and bottom right are (0,0), (315,0), (0,207) and (315,207) respectively. The midpoint of the green-pink rectangle pattern in R1 is approximately located at (157.5, 103.5). In order to estimate the location of R1 from Robot F's view field, two types of offsets are used; namely Offset A and Offset B. Offset A is the difference between the midpoints of the image coordinate and the pattern in x-axis, whereas Offset B shows the difference of midpoints in y-axis. By default, the offsets value will be zero when the pattern stays exactly in the middle of Robot F's view field. A negative or positive offset value indicates that Robot F needs to move until the pattern goes back to the default position within its view field. In this work, we set the tolerance at *±20* with respect to the middle point. Table I summarizes the location of the pattern when the offset values deviate from zero.

TABLE I. Pattern Locations When the Offset Values Deviate from Zero

Type of offset	Positive Difference (+ve)	Negative Difference (-ve)
Offset A	Pattern is located at the left-hand side of the captured image	Pattern is located at the right-hand side of the captured image
Offset B	Pattern is located above midpoint of the image captured	Pattern is located below midpoint of the image captured

A major limitation of the distance estimation technique via the visual servoing appears to be the tracking range. In this specific configuration, if the reference image gets too close to Robot F, the horizontal and vertical edges of the image will go beyond the view field. Hence the values of *x* and *y* cannot be extracted, which makes it impossible to calculate the estimated distance *d*. This scenario is illustrated in Fig. 3. This scenario however may not be a major problem for distance estimation using S1 due to its capability to detect an obstacle in a small range.

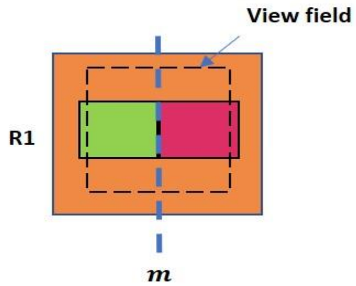

Figure 3. Illustration on the reference image as viewed by Robot F when its distance from Robot L is too close.

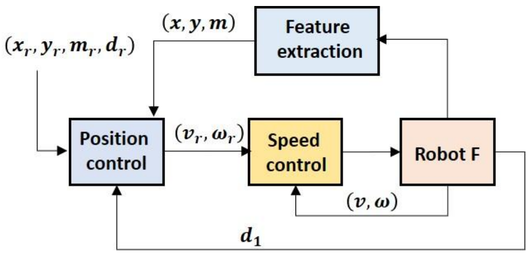

Figure 4. Speed and position control structure for Robot F.

With regard to Robot F's trajectory, a speed controller and a position controller are designed and embedded in the Robot F's microcontroller unit in such a way that the distance between Robot F and Robot L always stays within d_r cm, and the position of the reference image as viewed by Robot F is within a specified range (i.e. x_r, y_r and m_r). The values of x,y and m extracted from the image detected will also be utilized to calculate the corresponding distance between Robot F and Robot L. Hence, two distance values (one from S1 and another from S2) are available and will be fed back to the position controller to provide the desired linear and angular speeds (v_r and ω_r) for Robot F. The overall structure of the speed and position control strategy is shown in Fig. 4. Based on individual performance of each sensor, the estimated distance, denoted as d_a , is set equal to the distance detected by S2 when d_1>30cm, and $d_a = d_1$ when d_1<30cm. A Proportional-Integral controller is designed as the speed controller to adjust the speeds by minimizing the mismatch between (v_r,ω_r) and (v,ω). The speeds however are constrained between -20cm/s and 20cm/s for v_r, and -20rad/s and 20rad/s for ω_r. Experimental results are presented in the next section.

III. Experimental Results and Discussions

In this work, the design requirement is that Robot F needs to track and follow Robot L and stops when $15 \leq d_a \leq 18$ cm, and $(x,y,m)=(x_r,y_r,m_r)$. Two initial conditions are considered to evaluate the tracking performance of Robot F; the first one (Condition 1) is when both robots are initially on a straight line where Robot F is facing the back of Robot L as in Fig. 1, and the second one (Condition 2) is when Robot L is initially not on the same line as Robot F.

For Condition 1, three different experiments are conducted as follows:

i. Experiment 1.1: Robot L is initially placed approximately 40cm in front of Robot F, and Robot L remains stationary.
ii. Experiment 1.2: Robot L is initially placed approximately 25cm in front of Robot F, and Robot L moves forward for 1 second and stops.
iii. Experiment 1.3: Robot L is initially placed approximately 15cm in front of Robot F, and Robot L moves backward for 0.5 second and stops.

The setups for Experiments 1.1, 1.2 and 1.3 are illustrated in Figs. 5, 6 and 7 respectively.

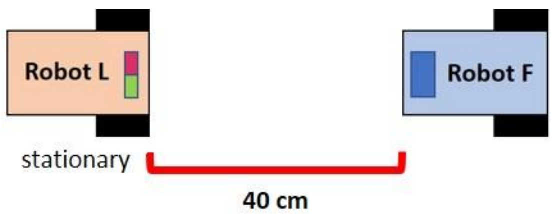

Figure 5. Illustration on the setup for experiment 1.1.

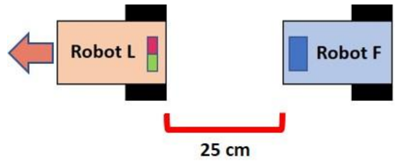

Figure 6. Illustration on the setup for Experiment 1.2.

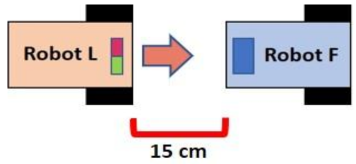

Figure 7. Illustration on the setup for Experiment 1.3.

Figs. 8, 9 and 10 show the speeds and the distance values detected by S1 (denoted as d_1) and S2 (denoted as d_2) for Experiments 1.1, 1.2 and 1.3 respectively. We can see that Robot F successfully tracked Robot L and eventually stopped when d_a is within the desired range. Fig. 7 shows that d_2 drops to zero. between t=1 and t=1.5 even when the true distance is not within the range. Robot F however did not stop as d_a is set to be dependent on d_1 when d_1<30 cm. The same trend can also be observed from Figs. 8 and 9 where S2 becomes ineffective in giving the correct distance value when both robots are sufficiently close to each other. The settling time, which is the time when Robot F successfully follows Robot L within the specified range for Experiments 1.1, 1.2 and 1.3 are tabulated in Table II.

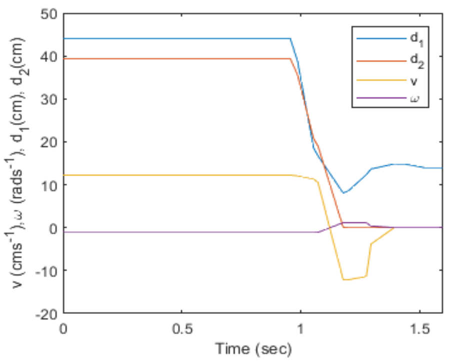

Figure 8. Experiment 1.1: Robot F moves forward towards Robot L and stops at t=1.40s. S2 reading drops to zero when both robots are sufficiently close to each other.

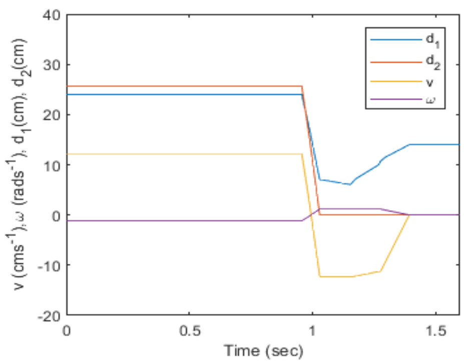

Figure 9. Experiment 1.2: Robot F moves towards a moving Robot L and stops at t=1.52s. S2 reading drops to zero when both robots are sufficiently close to each other.

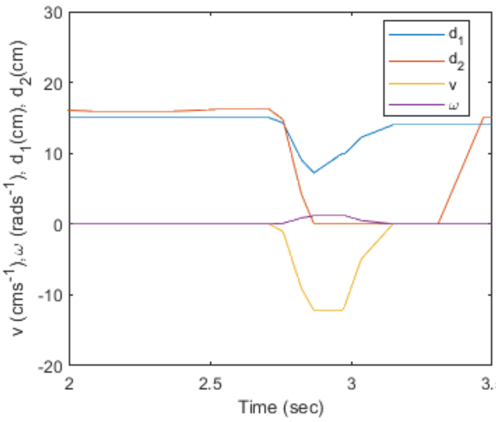

Figure 10. Experiment 1.3: Robot F moves backward and stops after 1.2s. S2 reading drops to zero when both robots are sufficiently close to each other.

TABLE II. SETTLING TIME FOR EXPERIMENTS 1.1, 1.2 AND 1.3

Trial	Settling time (s)		
	Exp. 1.1	Exp. 1.2	Exp. 1.3
1	1.40	1.45	1.20
2	1.39	1.10	1.00
3	1.28	2.20	1.01
Average	1.36	1.58	1.07

For Condition 2, two different experiments are conducted as follows:

i. Experiment 2.1: Robot L is placed at 15° to the left of Robot F, and 30cm away. Robot L remains stationary.

ii. Experiment 2.2: Robot L is placed at 15° to the right of Robot F, and 30cm away. Robot L remains stationary.

The setups for Experiments 2.1 and 2.2 are illustrated in Figs. 11 and 12 respectively.

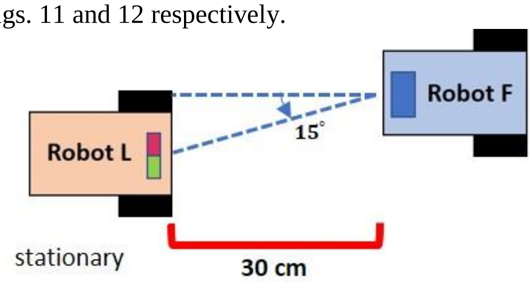

Figure 11. Illustration on the setup for Experiment 2.1.

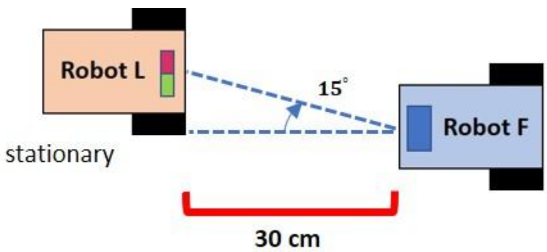

Figure 12. Illustration on the setup for Experiment 2.2.

The speed and distance values for Experiment 2.1 are shown in Fig. 13, and the corresponding value of Offset A is shown in Fig. 14. In this case, Robot F successfully tracked Robot L and stopped when d_a is within the desired range. It is also observed that the value of Offset A started with a positive value, indicating that Robot L was initially at the right hand side of Robot F. Robot F then moved until the Offset A value was driven into the tolerance of ± 20.

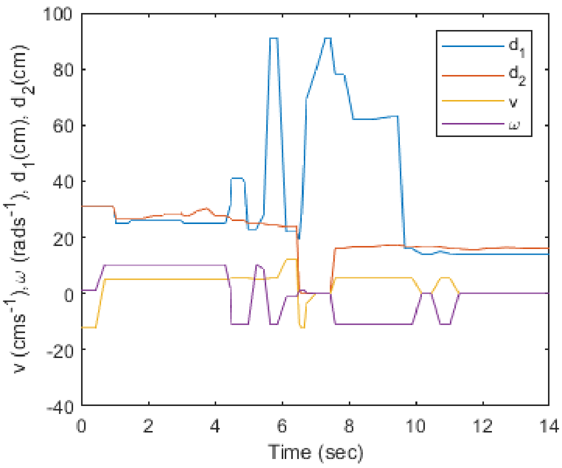

Figure 13. Experiment 2.1: Robot F steers towards Robot L and stops at t=11.5s. S1 reading overshoots for approximately 5 seconds.

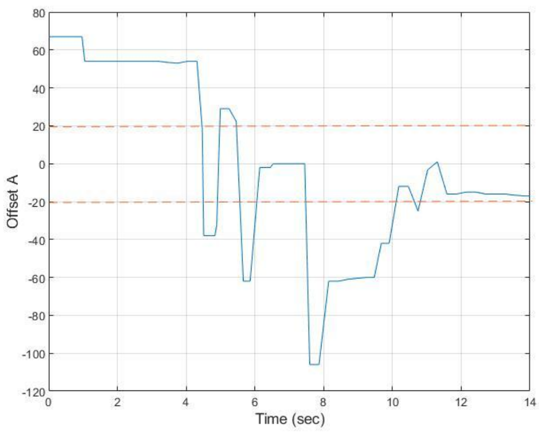

Figure 14. Experiment 2.1: The offset value as Robot F moves towards Robot L.

For Experiment 2.2, the responses are shown in Figs. 15 and 16, and we can see a quite similar performance as in Experiment 2.1. In this case, the value of Offset A started with a negative value, indicating that Robot L was initially at the left hand side of Robot F.

In both experiments, S2 provides a more accurate reading as compared to S1, and S1 tends to output values that are clearly out of range. The settling time for both experiments are tabulated in Table III.

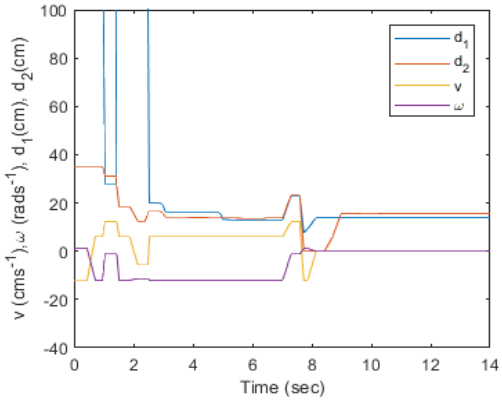

Figure 15. Experiment 2.2: Robot F steers towards Robot L and stops at t=8.5s. S1 reading overshoots for approximately 3 seconds.

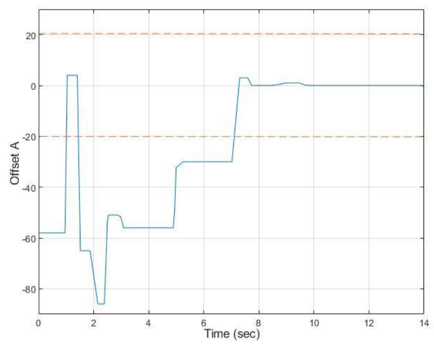

Experiment 2.2: The offset value as Robot F moves towards Robot L.

TABLE III. SETTLING TIME FOR EXPERIMENTS 2.1 AND 2.2

Trial	Settling time (s)	
	Exp. 2.1	Exp. 2.2
1	11.40	9.45
2	9.51	9.10
3	10.90	10.20
Average	10.6	9.58

We define the compensation duration as the time when S1 reads the correct values (within the tolerance) while S1 does not, and vice versa. The compensation duration for all experiments are recorded in Table III, and it is shown that both sensors compensate each other's limitations with average time between 0.23s and 0.37s for Experiments 1.1 to 1.3, and between 3.53s and 4.13s.

TABLE IV. COMPENSATION DURATION FOR ALL EXPERIMENTS

Trial	Compensation Duration (s)				
	Exp. 1.1	Exp. 1.2	Exp. 1.3	Exp. 2.1	Exp. 2.2
1	0.3	0.4	0.2	5.2	4.1
2	0.4	0.4	0.3	4.1	3.5
3	0.4	0.4	0.2	3.1	3.0
Average	0.37	0.4	0.23	4.13	3.53

IV. CONCLUSIONS AND FUTURE WORKS

In this work, we have developed a framework for a hybrid sensor system consisting of an image sensor and a range sensor to improve the PBVS technique of an autonomous wheeled mobile robot. Two mini nonholonomic robots are used as the test beds and a set of experiments is designed in this work to investigate the impacts of the hybrid sensor system on the tracking performance of the robot. Experimental results show that the image sensor loses its detection when the target image is too close, while the range sensor produces unreliable readings when the target object is sufficiently far and not in the line of sight. With the speed of the robots constrained within ±20 cm/s, and distance between them not more than 40cm, it is shown that both sensors compensate each other's limitations in order to ensure the tracking performance is within the design requirement.

For future works, the reference image's size or pattern can be optimized in order to allow a longer tracking range. The visual servoing technique from the proposed framework may also be further improved by enhancing the performance of the algorithm for the feature extractions and speed control strategy to minimize the settling time.

ACKNOWLEDGEMENTS

The authors would like to thank Universiti Sains Malaysia for the financial support under Short Term Grant (304/PELECT/60313018).

REFERENCES

[1] S. Hutchinson, G. D. Hager, P. I. Corke, "Tutorial on visual servo control," *IEEE Transactions on Robotics and Automation*, vol. 12, no. 5, pp. 651–670, 1996.

[2] G. J. Agin, "Real time control of a robot with a mobile camera," *SRI International*, Menlo Park, 1979.

[3] J. T. Feddema and O. R. Mitchell, "Vision-guided servoing with feature-based trajectory generation," *IEEE Transactions on Robotics and Automation*, vol. 5, no. 5, pp. 691–700, 1989.

[4] G. L. Mariottini, G. Oriolo, D. Prattichizzo, "Image-based visual servoing for nonholonomic mobile robots using epipolar geometry," *IEEE Transactions on Robotics*, vol. 23, no. 1, pp. 87–100, 2007.

[5] F. Chaumette, "Potential problems of stability and convergence in image-based and position-based visual servoing," In: Kriegman D.J., Hager G.D., Morse A.S. (eds) The confluence of vision and control. Lecture Notes in Control and Information Sciences, vol 237. Springer, London, 1998.

[6] W. Wilson, "Visual servo of robots using Kalman filter estimates of robot pose relative to a work-pieces," in: K. Hashimoto (Ed.), Visual Servoing, World Scientific, Singapore, 1994, pp. 71–104.

[7] V. Lippiello, B. Siciliano, and L. Villani, "Position-based visual servoing in industrial multirobot cells using a hybrid camera configuration," *IEEE Transactions on Robotics*, vol. 23, no. 1, pp. 73-86, Feb. 2007.

[8] K. Sunhyo and Se-Young Oh, "Hybrid position and image based visual servoing for mobile robots," *Journal of Intelligent and Fuzzy Systems*, vol. 18, pp. 73-82, 2007.